Plastic Hinge Integration Methods for Force-Based Beam–Column Elements

Michael H. Scott[1] and Gregory L. Fenves[2]

Abstract: A new plastic hinge integration method overcomes the problems with nonobjective response caused by strain-softening behavior in force-based beam–column finite elements. The integration method uses the common concept of a plastic hinge length in a numerically consistent manner. The method, derived from the Gauss–Radau quadrature rule, integrates deformations over specified plastic hinge lengths at the ends of the beam–column element, and it has the desirable property that it reduces to the exact solution for linear problems. Numerical examples show the effect of plastic hinge integration on the response of force-based beam–column elements for both strain-hardening and strain-softening section behavior in the plastic hinge regions. The incorporation of a plastic hinge length in the element integration method ensures objective element and section response, which is important for strain-softening behavior in reinforced concrete structures. Plastic rotations are defined in a consistent manner and clearly related to deformations in the plastic hinges.

DOI: 10.1061/(ASCE)0733-9445(2006)132:2(244)

CE Database subject headings: Beam columns; Finite elements; Earthquake engineering; Nonlinear analysis; Plastic hinges; Simulation models.

Introduction

The advent of performance-based earthquake engineering has placed an emphasis on simulating the nonlinear response of a structural system to seismic excitations (Filippou and Fenves 2004). Severe earthquake ground motions are expected to deform a structure into the inelastic range of behavior through multiple excursions. The design of a structural system subjected to earthquake ground motion recognizes that plastic hinges will form in frame members. Accurate and computationally efficient numerical models that represent the cyclic loading of plastic hinges in beam–column elements, including the effect of degradation, are thus required to simulate the seismic response and evaluate the performance of structural systems.

Finite element models for the nonlinear material response of beam–column members have fallen into two categories: concentrated plasticity and distributed plasticity. In concentrated plasticity, the nonlinear behavior of a beam–column member is lumped into rotational springs at the ends of a linear-elastic element. The two-component model (Clough et al. 1965) and the one-component model (Giberson 1967) are the most common approaches for concentrated plasticity beam–column elements. The concentrated plasticity concept was generalized to incorporate axial-moment interaction at the element ends (Hilmy and Abel 1985; Powell and Chen 1986). The drawback to concentrated plasticity models, however, is they separate axial-moment interaction from the element behavior. Consequently, a beam–column element requires a calibration based on the expected axial load and moment gradient along the member.

Distributed plasticity beam–column elements are based on the displacement- or force-based formulation, both of which allow plastic hinges to form at any location and account for axial-moment interaction by integrating the force-deformation response at sections along the element length. The behavior at a section is described by a fiber model or a stress resultant plasticity model (El-Tawil and Deierlein 1998). The number of sections and their location is determined by the numerical quadrature rule, such as those based on Gauss quadrature, used to integrate the element force-deformation relationship. Displacement-based beam–column elements follow the standard finite element approach, in which the element displacement field is expressed as a function of the nodal displacements (Hughes 1987; Zienkiewicz and Taylor 2000). The displacement field is approximate, thus several displacement-based elements are required along the length of a frame member to represent the deformations in a plastic hinge region. In contrast, force-based beam–column elements interpolate the section forces in terms of the basic forces, satisfying equilibrium even in the range of nonlinear material response (Spacone et al. 1996). The advantages of force-based beam–column elements over displacement-based elements have been discussed by Neuenhofer and Filippou (1997). The primary advantage is the ability to use one force-based element to simulate the material nonlinear response of a frame member, compared with several displacement-based elements, thereby keeping the number of degrees of freedom in the structural model to a minimum.

The strain-softening behavior of concrete can cause localization in beam–column elements, particularly in the simulation of reinforced concrete columns that carry high gravity loads. Localized response in reinforced concrete members modeled by

[1]Assistant Professor, Dept. of Civil, Construction, and Environmental Engineering, Oregon State Univ., Corvallis, OR 97331 (corresponding author). E-mail: michael.scott@oregonstate.edu

[2]Professor, Dept. of Civil and Environmental Engineering, Univ. of California, Berkeley, CA 94720. E-mail: fenves@berkeley.edu

Note. Associate Editor: Keith D. Hjelmstad. Discussion open until July 1, 2006. Separate discussions must be submitted for individual papers. To extend the closing date by one month, a written request must be filed with the ASCE Managing Editor. The manuscript for this paper was submitted for review and possible publication on October 26, 2004; approved on March 24, 2005. This paper is part of the ***Journal of Structural Engineering***, Vol. 132, No. 2, February 1, 2006. ©ASCE, ISSN 0733-9445/2006/2-244–252/$25.00.

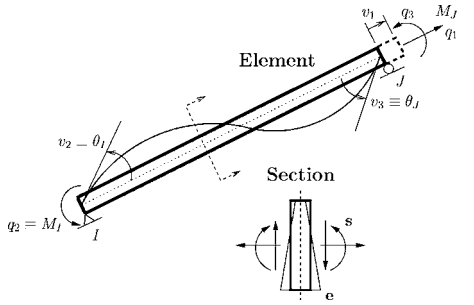

Fig. 1. Simply supported basic system for two-dimensional beam–column elements and cross section of element

continuum finite elements was investigated by de Borst et al. (1994) and Bazant and Planas (1998). Consistent with their findings in the continuum context, the displacement-based approach causes localization of response over a single displacement-based beam–column element. The length of the element undergoing softening response controls the structural response, thus leading to nonobjectivity because the structural response depends on the choice of the characteristic length in the finite element discretization. In contrast, with force-based beam–column elements deformations localize at a single integration point rather than across an entire element, making the characteristic length equal to the integration weight associated with the section undergoing strain softening. This leads to a loss of objectivity because the response changes as a function of the number of element integration points rather than as a function of the element length. To address localization in force-based elements, Coleman and Spacone (2001) developed a constant fracture energy regularization technique to maintain objective response for strain-softening behavior as the number of integration points changes. This regularization method, however, requires a modification of the stress–strain properties in the element based on the number of integration points.

To address this problem, this paper presents a new element integration method that confines nonlinear constitutive behavior to plastic hinge regions of a specified length while maintaining numerical accuracy and objectivity. The force-based formulation is ideal for this approach because the deformations in the plastic hinge regions are computed such that the corresponding section forces are in equilibrium with the element end forces. The paper begins with the force-based beam–column element using the standard Gauss–Lobatto integration rule for distributed plasticity. Then, the concept of plastic hinge integration is presented. Three plastic hinge integration methods are investigated to arrive at a new, optimal approach based on Gauss–Radau quadrature. This paper concludes with numerical examples that demonstrate the differences between the plastic hinge integration methods and show how the inclusion of a plastic hinge length in the element integration rule enables objective response for the beam–column sections, element, and ultimately the structure.

Force-Based Element Formulation

Force-based beam-column elements (Spacone et al. 1996) are formulated in a basic system without rigid-body displacement modes. The element deformations, in the vector $\mathbf{v}$, are assumed small compared to the element length. There are three element deformations for two-dimensional elements, as shown in Fig. 1 for a simply supported basic system, and six for three-dimensional elements. The vector of forces in the basic system, $\mathbf{q}=\mathbf{q}(\mathbf{v})$, is a function of the element deformations. The section behavior is expressed in terms of the section deformations, $\mathbf{e}$, and the corresponding section forces, $\mathbf{s}=\mathbf{s}(\mathbf{e})$. The element kinematic relationship is assumed linear in this paper, but it can be extended to large displacements.

Equilibrium between the basic and section forces is expressed in strong form as

$$\mathbf{s}=\mathbf{b}\mathbf{q} \tag{1}$$

where the matrix $\mathbf{b}$ contains interpolation functions relating section forces to basic forces from equilibrium of the basic system. The axial force and bending moment at location x along the element for a two-dimensional simply supported basic system is given by the following equilibrium interpolation matrix:

$$\mathbf{b}=\begin{bmatrix} 1 & 0 & 0 \\ 0 & x/L-1 & x/L \end{bmatrix} \tag{2}$$

Eqs. (1) and (2) can be extended to include member loads and section shear. From the principle of virtual forces, the compatibility relationship between the section and element deformations is

$$\mathbf{v}=\int_0^L \mathbf{b}^T\mathbf{e}\,dx \tag{3}$$

The linearization of Eq. (3) with respect to the basic forces gives the element flexibility matrix

$$\mathbf{f}=\frac{\partial \mathbf{v}}{\partial \mathbf{q}}=\int_0^L \mathbf{b}^T\mathbf{f}_s\mathbf{b}\,dx \tag{4}$$

The section stiffness matrix is $\mathbf{k}_s=\partial\mathbf{s}/\partial\mathbf{e}$, and its inverse gives the section flexibility matrix, $\mathbf{f}_s=\mathbf{k}_s^{-1}$. The element stiffness matrix, $\mathbf{k}$, in the basic system is the inverse of the element flexibility matrix, $\mathbf{k}=\mathbf{f}^{-1}$, as given in Eq. (4). Details of the implementation of the force-based beam–column element for use in a general finite element analysis framework using the direct stiffness method are given by Neuenhofer and Filippou (1997).

The compatibility relationship in Eq. (3) is evaluated by numerical quadrature

$$\mathbf{v}=\sum_{i=1}^{N_p}(\mathbf{b}^T\mathbf{e}|_{x=\xi_i})\omega_i \tag{5}$$

where ξ and ω=locations and associated weights, respectively, of the N_p integration points over the element length $[0,L]$. In a similar manner, the element flexibility matrix in Eq. (4) is evaluated numerically

$$\mathbf{f}=\sum_{i=1}^{N_p}(\mathbf{b}^T\mathbf{f}_s\mathbf{b}|_{x=\xi_i})\omega_i \tag{6}$$

Gauss–Lobatto quadrature is used in force-based elements because it places integration points at the element ends, where the bending moments are largest in the absence of member loads. A graphical representation of the four-point ($N_p=4$) Gauss–Lobatto quadrature rule applied to Eq. (5) is shown in Fig. 2, where the integrand, $\mathbf{b}^T\mathbf{e}$, is evaluated at the ith location ξ_i and treated as constant over the length ω_i. The highest order polynomial integrated exactly by the Gauss–Lobatto quadrature rule is $2N_p$-3, which is two orders lower than Gauss–Legendre quadrature (Hildebrand 1974). For a linear-elastic, prismatic beam–column element without member loads, quadratic polynomials appear in the integrand of Eq. (3) due to the product of the linear curvature

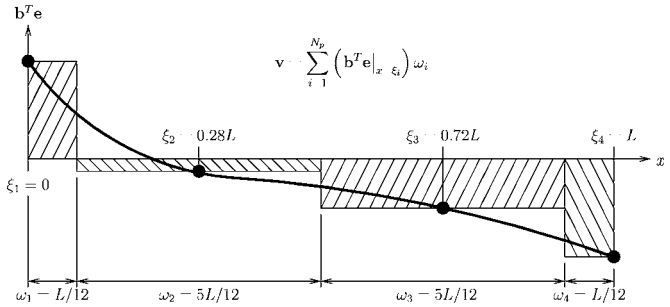

Fig. 2. Application of four-point Gauss–Lobatto quadrature rule to evaluate force-based element compatibility relationship

distribution in the vector **e** with the linear interpolation functions for the bending moment in the matrix **b**. Therefore, at least three Gauss–Lobatto integration points are required to represent exactly a linear curvature distribution along the element. To represent accurately the nonlinear material response of a force-based beam–column element, four to six Gauss–Lobatto integration points are typically used (Neuenhofer and Filippou 1997).

Loss of Objectivity in Force-Based Beam–Column Elements

The primary advantage of the Gauss–Lobatto integration rule is it permits the spread of plasticity along the element length. For hardening section behavior, the computed element response will converge to a unique solution as the number of integration points increases. On the other hand, for softening section behavior where deformations localize at a single integration point, a unique solution does not exist and the computed response depends on the characteristic length implied by the integration weights of the Gauss–Lobatto quadrature rule. This leads to a loss of objectivity, where the element response will change as a function of N_p.

To address the loss of objectivity in force-based beam–column elements, Coleman and Spacone (2001) developed a regularization technique that modifies the material stress–strain behavior to maintain a constant energy release after strain-softening initiates. Coleman and Spacone applied this method to the Kent–Park concrete model (Kent and Park 1971) shown in Fig. 3, where the shaded area is equal to the energy released after the onset of strain softening

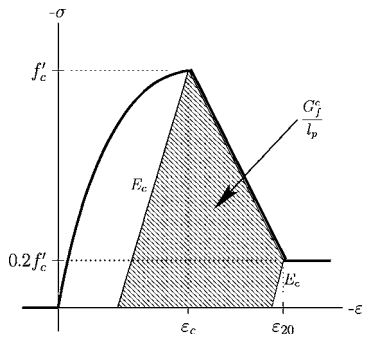

Fig. 3. Kent–Park concrete stress–strain model with fracture energy in compression as shaded area

$$\frac{G_f^c}{l_p} = 0.6f_c'\left(\varepsilon_{20} - \varepsilon_c + \frac{0.8f_c'}{E_c}\right) \tag{7}$$

The parameters for the Kent–Park concrete model are f_c'=concrete compressive strength; ε_c=peak compressive strain; E_c=elastic modulus; and ε_{20}=strain corresponding to 20% of the compressive strength. The parameter G_f^c=concrete fracture energy in compression, and l_p=plastic hinge length, which acts as the characteristic length for the purpose of providing objective response.

As discussed in the previous section, the plastic hinge length in the model is directly related to the element integration rule for force-based elements. For the l_p implied by the number of Gauss–Lobatto integration points, ε_{20} must be modified according to Eq. (7) in order to maintain a constant energy release

$$\varepsilon_{20} = \frac{G_f^c}{0.6f_c'l_p} - \frac{0.8f_c'}{E_c} + \varepsilon_c \tag{8}$$

Although this approach maintains objective response at the global level, it affects the local section response through an unnatural coupling of the concrete material properties to the element integration rule. A second regularization is required to correct for the loss of objectivity in the section response that results from this approach (Coleman and Spacone 2001).

For the plastic hinge integration methods presented in this paper, l_p is specified as part of the element integration rule and it becomes a free parameter. Therefore, it is possible to determine a plastic hinge length that will maintain a constant energy release without modification to the concrete stress-strain relationship, alleviating the need for a subsequent regularization of the section response. For example, using the approach of Coleman and Spacone, the plastic hinge length can be determined from the concrete properties using Eq. (7)

$$l_p = \frac{G_f^c}{0.6f_c'(\varepsilon_{20} - \varepsilon_c + 0.8f_c'/E_c)} \tag{9}$$

The introduction of a plastic hinge length, such as that computed by Eq. (9), to the element integration rule maintains the logical separation of the material properties from the element integration rule.

Alternatively, the plastic hinge length can be specified using an empirically validated relationship, such as the Paulay and Priestley (1992) equation for reinforced concrete members

$$l_p = 0.08L + 0.022f_y d_b \text{ (kN, mm)} \tag{10}$$

where L=length of the member; and f_y and d_b=yield strength and diameter, respectively, of the longitudinal reinforcing bars. The advantage of this approach is that the plastic hinge length includes the effect of strain softening and localization as determined by experiments.

Plastic Hinge Integration Methods

The specification of a plastic hinge length in the element integration rule, whether computed by Eqs. (9), (10), or other means, is investigated in this section to achieve objectivity for softening response. The plastic hinge integration methods presented herein are based on the assumption that nonlinear constitutive behavior is confined to regions of length l_{pI} and l_{pJ} at the element ends. As such, the elements are useful for columns or beams that carry small member loads. To represent plastic hinges in force-based

beam–column elements, the compatibility relationship in Eq. (3) is separated into three integrals, one for each hinge region and one for the interior region of the element

$$\mathbf{v} = \int_0^{l_{pI}} \mathbf{b}^T \mathbf{e}\, dx + \int_{l_{pI}}^{L-l_{pJ}} \mathbf{b}^T \mathbf{e}\, dx + \int_{L-l_{pJ}}^{L} \mathbf{b}^T \mathbf{e}\, dx \tag{11}$$

The section deformations are integrated numerically over the plastic hinge regions, whereas the contribution of the element interior is assumed to be linear elastic and evaluated by the flexibility of the interior region

$$\mathbf{v} = \sum_{i=1}^{N_p} (\mathbf{b}^T \mathbf{e}|_{x=\xi_i})\omega_i + \mathbf{f}_{\text{int}}^e \mathbf{q} \tag{12}$$

where ξ and ω=locations and associated weights, respectively, of the N_p integration points in the plastic hinge regions. The flexibility matrix of the element interior region, $\mathbf{f}_{\text{int}}^e$, is evaluated by the closed-form integral

$$\mathbf{f}_{\text{int}}^e = \int_{l_{pI}}^{L-l_{pJ}} \mathbf{b}^T \mathbf{f}_s^e \mathbf{b}\, dx \tag{13}$$

The matrix $\mathbf{f}_s^e$ contains the elastic flexibility coefficients at a cross section of the interior

$$\mathbf{f}_s^e = \begin{bmatrix} \dfrac{1}{EA} & 0 \\ 0 & \dfrac{1}{EI} \end{bmatrix} \tag{14}$$

with the elastic modulus E, the cross-sectional area A, and the second moment of the cross-sectional area I. Eq. (14) assumes the coordinate axis is located at the centroid of the section. The linearization of Eq. (12) with respect to the basic forces gives the element flexibility as the sum of numerical integration over the plastic hinge regions and the flexibility of the element interior

$$\mathbf{f} = \sum_{i=1}^{N_p} (\mathbf{b}^T \mathbf{f}_s \mathbf{b}|_{x=\xi_i})\omega_i + \mathbf{f}_{\text{int}}^e \tag{15}$$

As a limiting case, the numerical integration for distributed plasticity in Eqs. (5) and (6) is recovered from Eqs. (12) and (15) when the sum of the plastic hinge lengths is equal to the element length, $l_{pI}+l_{pJ}=L$. In this case, the matrix $\mathbf{f}_{\text{int}}^e$ is zero.

To represent strain softening in the plastic hinge regions of the element, it is desirable to use a plastic hinge integration rule for Eqs. (12) and (15) that satisfies the following criteria:

1. Sample section forces at the element ends where the bending moments are largest in the absence of member loads;
2. Integrate quadratic polynomials exactly to provide the exact solution for linear curvature distributions; and
3. Integrate deformations over the specified lengths l_{pI} and l_{pJ} using a single section in each plastic hinge region.

The Gauss–Lobatto integration rule for distributed plasticity satisfies criteria (1) and (2), but it does not satisfy (3) because the plastic hinge lengths are implied by the number of integration points, N_p. Note that if an integration rule satisfies the three criteria, strain hardening can be represented, but it does not spread past the specified plastic hinge lengths. In the following subsections, three plastic hinge integration methods are investigated to arrive at a fourth method that meets the three criteria for strain-softening response.

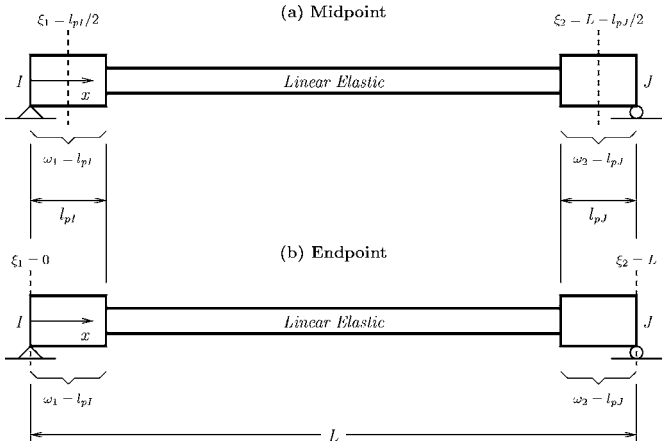

Fig. 4. Midpoint and endpoint plastic hinge integration methods

Midpoint Integration

The most accurate one-point integration method is the midpoint rule, for which the integration points are located at the center of each plastic hinge region, $\xi=\{l_{pI}/2, L-l_{pJ}/2\}$, and the weights are equal to the plastic hinge lengths, $\omega=\{l_{pI}, l_{pJ}\}$. The midpoint rule is illustrated in Fig. 4(a). A major drawback to the midpoint rule is the integration points are not located at the element ends where the maximum bending moments occur in the absence of member loads. As a result, the element will exhibit a larger flexural capacity than expected, which in fact will be a function of the plastic hinge lengths. Furthermore, the midpoint rule gives the exact integration of only linear functions, thus there is an error in the integration of quadratic polynomials. In summary, the midpoint plastic hinge integration method satisfies criterion (3), but not (1) or (2).

Endpoint Integration

The integration points can be located at the element ends, $\xi=\{0, L\}$, while the integration weights remain equal to the plastic hinge lengths, $\omega=\{l_{pI}, l_{pJ}\}$, as shown in Fig. 4(b). However, an order of accuracy is lost with this endpoint integration approach, because it is only capable of the exact integration of constant functions, which produces a significant error in the representation of linear curvature distributions. Therefore, the endpoint plastic hinge integration method meets criteria (1) and (3), but it fails (2).

Two-Point Gauss–Radau Integration

From the previous two methods, it is not possible to perform one-point integration for each plastic hinge region and satisfy the three criteria. As a result, it is necessary to investigate two-point integration methods. Two-point Gauss–Legendre integration over each plastic hinge region gives the desired level of element integration accuracy; however, there are no integration points at the element ends. Two-point Gauss–Lobatto integration over the hinge regions places integration points at the element ends, but is not exact for the case of a linear curvature distribution.

An alternative two-point integration rule is based on Gauss–Radau quadrature (Hildebrand 1974). It is similar to Gauss–Lobatto, but it has an integration point at only one end of an interval rather than at both ends. This gives Gauss–Radau quadrature an accuracy of $2N_p-2$, one order higher than that for Gauss–

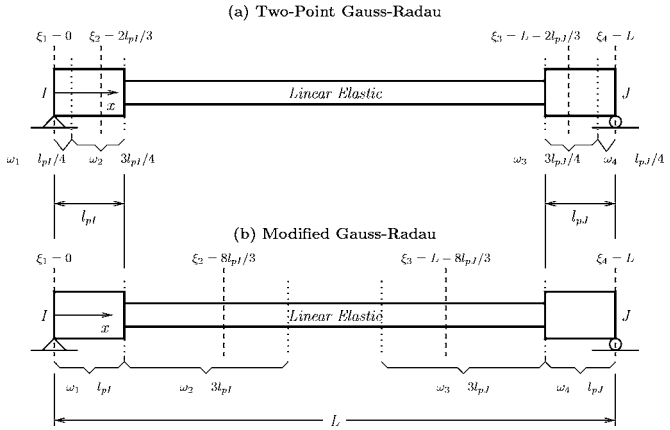

Fig. 5. Two-point Gauss–Radau and modified Gauss–Radau plastic hinge integration methods

Lobatto. As a result, two Gauss–Radau integration points in each plastic hinge region gives the exact integration for an element with a linear curvature distribution.

On the interval [0,1], the two-point Gauss–Radau integration rule has integration points at $\{0,2/3\}$ with corresponding integration weights $\{1/4,3/4\}$. The mapping of this integration rule to the plastic hinge regions at the element ends gives four integration points, $\xi=\{0,2l_{pI}/3,L-2l_{pJ}/3,L\}$, along with their respective weights, $\omega=\{l_{pI}/4,3l_{pI}/4,3l_{pJ}/4,l_{pJ}/4\}$, as shown in Fig. 5(a).

There are two properties to note regarding the two-point Gauss–Radau integration rule. First, when the sum of the plastic hinge lengths is equal to the element length ($l_{pI}+l_{pJ}=L$) this integration rule becomes a four-point distributed plasticity method with integration points at the element ends. Second, Simpson's 3/8 integration rule (Stoer and Bulirsch 1993) is recovered when $l_{pI}=l_{pJ}=L/2$, increasing the accuracy by one order to the exact integration of cubic polynomials.

This integration method satisfies criteria (1) and (2). Criterion (3), however, is not satisfied, because strain softening will result in localization within the plastic hinge region. The characteristic length over which the localized deformations are integrated will be equal to the integration weight, $l_p/4$, assigned to the integration point at the element end rather than the plastic hinge length, l_p. This reduction in the characteristic length will cause the element to unload at a faster rate than expected to maintain equilibrium.

Modification of Two-Point Gauss–Radau Integration

To ensure localized deformations are integrated over the specified plastic hinge lengths, it is desirable to make the integration weights at the element ends equal to l_{pI} and l_{pJ} rather than $l_{pI}/4$ and $l_{pJ}/4$. To this end, the two-point Gauss–Radau integration rule is applied over lengths of $4l_{pI}$ and $4l_{pJ}$ at the element ends, as shown in Fig. 5(b), thus giving the integration point locations and weights

$$\xi=\{0,8l_{pI}/3,L-8l_{pJ}/3,L\}$$

$$\omega=\{l_{pI},3l_{pI},3l_{pJ},l_{pJ}\} \tag{16}$$

To confine nonlinear constitutive behavior to only the integration points at the element ends, the section response at the two interior integration points is assumed linear elastic, with the same properties as those defined in Eq. (14) for the element interior. As a result, the lower and upper limits of integration in Eq. (13) become $4l_{pI}$ and $L-4l_{pJ}$, respectively, and the elastic flexibility of the element interior is then the sum of three parts

$$\mathbf{f}_{\text{int}}^e=(\mathbf{b}^T\mathbf{f}_s^e\mathbf{b}|_{x=8/3l_{pI}})3l_{pI}+\int_{4l_{pI}}^{L-4l_{pJ}}\mathbf{b}^T\mathbf{f}_s^e\mathbf{b}\,dx+(\mathbf{b}^T\mathbf{f}_s^e\mathbf{b}|_{x=L-8/3l_{pJ}})3l_{pJ} \tag{17}$$

With this modification of Gauss–Radau, plasticity is confined to a single integration point at each end of the element. The representation of linear curvature distributions is exact, including the case where $4l_{pI}+4l_{pJ}>L$, because a definite integral is additive over its limits of integration. Furthermore, the characteristic length will be equal to the specified plastic hinge length when deformations localize due to strain-softening behavior in the hinge regions. Thus, all three criteria, (1), (2), and (3), are met by the present modification of the two-point Gauss–Radau plastic hinge integration method for force-based beam–column elements.

Computation of Plastic Rotations

The plastic rotations of a beam–column are an important demand parameter in assessing the response and damage of a structure to earthquakes or other loads causing the formation of plastic hinges. Emerging performance-based earthquake engineering specifications limit plastic rotation depending on the type of member and desired performance state (FEMA 2000). Therefore, it is essential that plastic rotations of a beam–column element be computed in a consistent manner. The force-based formulation is ideal for the computation of plastic rotations because the compatibility relationship in Eq. (12) is a summation of contributions from the plastic hinges and the elastic deformations of the element interior. This is in contrast with the displacement-based formulation, where the plastic rotations are dictated by the boundary values of the assumed transverse displacement field. Furthermore, since several displacement-based elements are required for a single member, it is very difficult to compute the plastic rotation, which is a response quantity for the member.

To compute the plastic rotations, the element deformation vector is decomposed into elastic and plastic components, $\mathbf{v}=\mathbf{v}^e+\mathbf{v}^p$. The plastic component is thus the difference between the total deformation of the member and the elastic component,

$$\mathbf{v}^p=\mathbf{v}-\mathbf{f}^e\mathbf{q} \tag{18}$$

in which the elastic component, $\mathbf{v}^e=\mathbf{f}^e\mathbf{q}$, is defined as the unloading of the element with the initial stiffness matrix, $\mathbf{k}^e=(\mathbf{f}^e)^{-1}$. This definition of plastic rotation, illustrated in Fig. 6, is consistent with the splitting of elastic and plastic strain in continuum mechanics (Simo and Hughes 1998). The matrix $\mathbf{f}^e$ is computed as the sum of the elastic contributions from the element interior and the hinge regions, $\mathbf{f}^e=\mathbf{f}_{\text{int}}^e+\mathbf{f}_{\text{hinge}}^e$. After substitution of Eq. (12) into Eq. (18), the plastic component of deformation (rotations and axial deformation) for a force-based beam–column element is

$$\mathbf{v}^p=\sum_{i=1}^{N_p}(\mathbf{b}^T\mathbf{e}|_{x=\xi_i})\omega_i-(\mathbf{f}^e-\mathbf{f}_{\text{int}}^e)\mathbf{q} \tag{19}$$

Eq. (19) applies to the plastic hinge integration methods presented in this paper, as well as to distributed plasticity integration by the Gauss–Lobatto rule, in which case the matrix $\mathbf{f}_{\text{int}}^e$ is zero. Alternative definitions of the plastic deformations are possible, such as the case where the element unloads from its current state, incor-

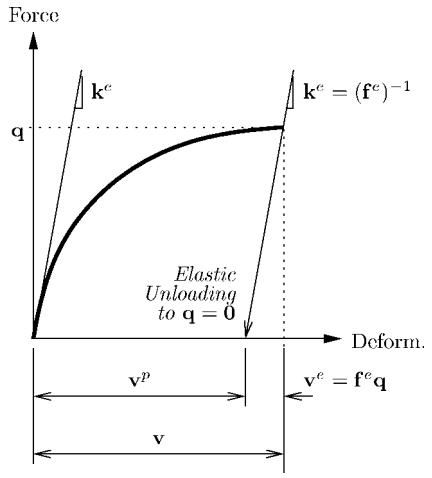

Fig. 6. Plastic deformations in beam–column element defined by unloading element with elastic stiffness matrix

porating degradation of the initial stiffness matrix. However, the implementation of alternative definitions of the unloading stiffness is more difficult.

For the modified Gauss–Radau plastic hinge integration method defined in the previous section, Eq. (19) sheds light on the relationship between plastic rotations and the plastic hinge lengths l_{pI} and l_{pJ}. The extraction of the elastic flexibility in the hinge regions, $\mathbf{f}^e_{\text{hinge}}$, from Eq. (19) leads to the following expression for plastic deformations of the element:

$$\mathbf{v}^p = \sum_{i=1}^{N_p} (\mathbf{b}^T \mathbf{e}^p|_{x=\xi_i})\omega_i - (\mathbf{f}^e - \mathbf{f}^e_{\text{int}} - \mathbf{f}^e_{\text{hinge}})\mathbf{q} \tag{20}$$

in which $\mathbf{e}^p$ = vector of plastic section deformations obtained from decomposition of the section deformations into elastic and plastic components, $\mathbf{e} = \mathbf{e}^e + \mathbf{e}^p$. The sum of the elastic flexibility matrices that multiply $\mathbf{q}$ in Eq. (20) is equal to zero, giving a simple relationship for the plastic element deformations in terms of the plastic section deformations

$$\mathbf{v}^p = \sum_{i=1}^{N_p} (\mathbf{b}^T \mathbf{e}^p|_{x=\xi_i})\omega_i \tag{21}$$

In the modified Gauss–Radau plastic hinge integration method, plasticity is confined to the sections at the ends of the element ($x=0, L$), while there are no plastic deformations for the elastic interior sections ($x=8/3 l_{pI}, L-8/3 l_{pJ}$). As a result, the plastic deformations for the element reduce to

$$\mathbf{v}^p = (\mathbf{b}^T \mathbf{e}^p|_{x=0}) l_{pI} + (\mathbf{b}^T \mathbf{e}^p|_{x=L}) l_{pJ} \tag{22}$$

At the ends of the element, the flexural terms of the force interpolation matrix defined in Eq. (2) are either 0 or ±1. Therefore, the plastic rotations are the product of the plastic curvature, κ^p, and the associated plastic hinge length at each end of the element

$$\begin{bmatrix} \theta^p_I \\ \theta^p_J \end{bmatrix} = \begin{bmatrix} -\kappa^p|_{x=0} l_{pI} \\ \kappa^p|_{x=L} l_{pJ} \end{bmatrix} \tag{23}$$

Eq. (23) demonstrates that the plastic curvatures can be obtained through a scaling of the plastic rotations computed with the modified Gauss–Radau plastic hinge integration method. This simple relationship between plastic rotation for the element and the plastic curvature is a major advantage of the new integration method.

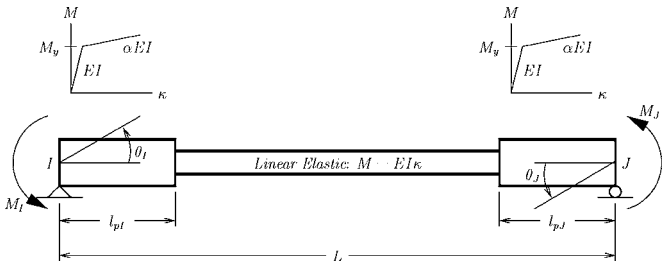

Fig. 7. Simply supported beam under state of antisymmetric bending with bilinear moment-curvature behavior in plastic hinge regions

Numerical Examples

The plastic hinge integration methods and plastic rotation computation for the force-based beam–column element formulation have been implemented in the *OpenSees* software framework system (McKenna et al. 2000). The numerical properties of the four plastic hinge integration methods for both hardening and softening flexural behavior in the hinge regions are investigated in the first example. The second example examines objectivity in the strain-softening response of a reinforced concrete bridge pier.

Comparison of Plastic Hinge Integration Methods

The moment-rotation response of the simply supported beam under antisymmetric bending shown in Fig. 7 demonstrates the differences in the four plastic hinge integration methods presented in this paper. A bilinear moment-curvature relationship describes the flexural behavior in the plastic hinge regions, where the elastic stiffness is EI, the yield moment is M_y, and strain hardening or softening is represented by the modulus αEI. The plastic hinge lengths l_{pI} and l_{pJ} are each set to $0.15L$ because a long plastic hinge length will highlight the differences between the integration methods.

The computed moment-rotation response of the beam using a single force-based element with the four plastic hinge integration methods is shown in Fig. 8(a) and compared with the closed-form solution for hardening flexural behavior with $\alpha = 0.03$ in the hinge regions. The yield moment computed with the midpoint integration method is greater than M_y because the bending moment is sampled at the center of the plastic hinge regions. As the rotation increases, the midpoint integration approaches the closed-form solution, showing the accuracy of the midpoint rule. The yield moment for the endpoint integration method is correct, but the elastic response is too flexible because of the large integration error. For the two-point Gauss–Radau integration method, the yield moment and elastic solution are exact. Of the four methods, it matches the closed-form solution the best because the hardening spreads across two integration points in the plastic hinge regions. For the modified Gauss–Radau method, the elastic solution and yield moment are exact. As seen in Fig. 8(a), however, the postyield response does not match the closed-form solution for hardening behavior because plasticity is confined to a single integration point at each end of the element.

The single integration point in each plastic hinge region with the modified Gauss–Radau method is beneficial for the case where deformations localize due to softening flexural behavior. The moment-rotation response for the beam with softening behavior ($\alpha = -0.03$) is shown in Fig. 8(b). When yielding occurs at the element ends, the flexural deformations localize at a single integration point, and the interior of the beam must unload to

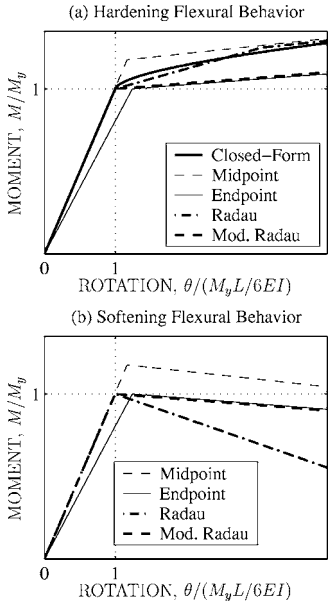

Fig. 8. Beam moment-rotation response resulting from plastic hinge integration for: (a) hardening flexural behavior and (b) softening flexural behavior

satisfy equilibrium. There is no unique solution for softening section behavior because the postyield response depends on the characteristic length over which the localized deformations are integrated. The postyield response is the same for the endpoint and the modified Gauss–Radau methods because in both cases the localized deformations occur at the element ends and are integrated over the characteristic length l_p. For the original two-point Gauss–Radau method the localized flexural deformations are integrated over a length of $l_p/4$, which is the integration weight at the element ends. This reduction in the characteristic length causes the beam to unload at a rate four times greater than that for the endpoint and modified Gauss–Radau integration methods.

Reinforced Concrete Bridge Pier

A reinforced concrete bridge pier, specimen 7 in the tests of Tanaka and Park (1990), is used in this example. The geometry and reinforcement details of the cantilever are shown in Fig. 9. The computed monotonic load-displacement response using one force-based element with Gauss–Lobatto integration and the new modified Gauss–Radau plastic hinge integration is compared with the envelope of the cyclic response from the experiment.

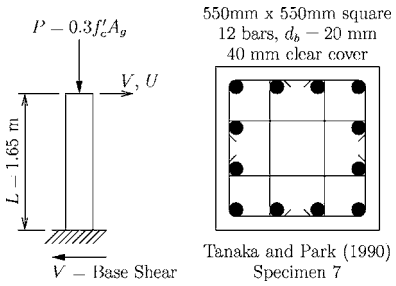

Fig. 9. Reinforced concrete bridge pier configuration and reinforcement details

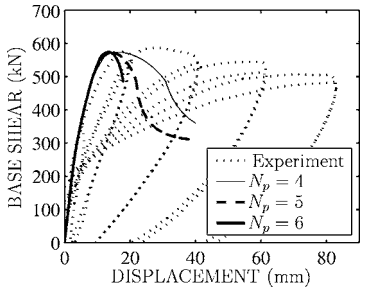

Fig. 10. Computed load-displacement response for reinforced concrete bridge pier with Gauss–Lobatto integration and nominal concrete properties

The compressive strength of the concrete is $f'_c = 32$ MPa. Due to the confining effects of the transverse reinforcement (Mander et al. 1988), the concrete properties in the core region are $f'_{cc} = 39$ MPa and $\varepsilon_{cc} = 0.0052$. In addition, $\varepsilon_{20} = 0.0248$ and $G^c_f = 180$ N/mm. The axial load applied to the pier is held constant at 30% of the gross section capacity. A bilinear stress–strain relationship is assumed for the reinforcing steel with elastic modulus, $E = 200{,}000$ MPa, yield stress, $f_y = 510$ MPa, and a 1% strain-hardening ratio. A fiber discretization of the pier cross section accounts for the concrete and steel stress–strain relationships and axial-moment interaction.

The computed response is shown in Fig. 10 for four, five, and six Gauss–Lobatto integration points with the nominal concrete properties. As seen in the figure, this is a poor approach to represent the envelope of the experimental response due to the rapid loss in postyield strength. In addition, the computed response is not objective because the rate of unloading varies greatly as the number of integration points increases.

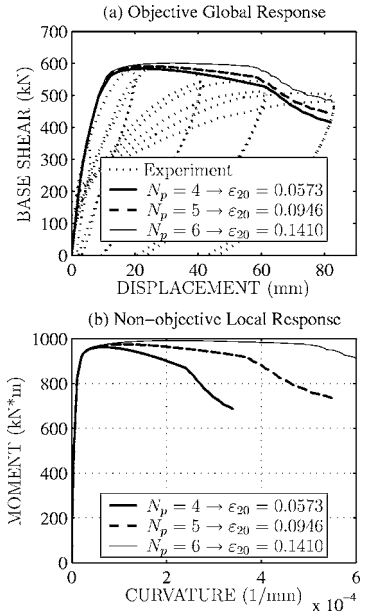

Fig. 11. Computed response for reinforced concrete bridge pier with Gauss–Lobatto integration: (a) objective results for global load-displacement response with modified concrete properties; (b) nonobjective results for moment-curvature response at base of bridge pier

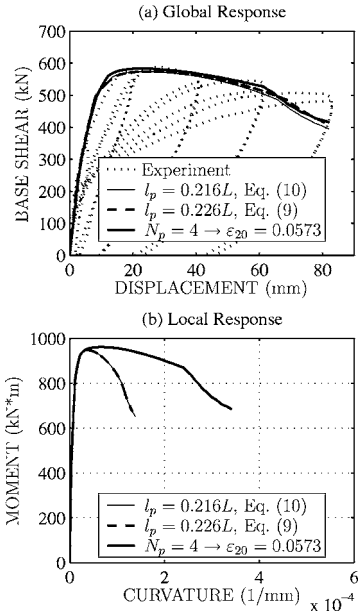

Fig. 12. (a) Global load-displacement response and (b) local moment-curvature response for reinforced concrete bridge pier with: (i) modified Gauss–Radau plastic hinge integration with l_p computed by Eq. (10); (ii) modified Gauss–Radau plastic hinge integration with l_p computed by Eq. (9); and (iii) four-point Gauss–Lobatto integration with modified concrete properties

To establish objectivity in the computed response, the concrete stress–strain parameter, ε_{20}, is modified according to Eq. (8) to maintain a constant energy release as the number of Gauss–Lobatto integration points changes (Coleman and Spacone 2001). For N_p=4, 5, and 6, the values of ε_{20} are 0.0573, 0.0946, and 0.1410, respectively. As seen in Fig. 11(a), the computed response matches the cyclic envelope of the experiment very well. The drawback to this approach, however, is the loss of objectivity in the moment-curvature response at the base of the bridge pier, as confirmed in Fig. 11(b). This loss of objectivity results from the modification of the concrete material properties to increase the curvature capacity of the section for the purpose of regularizing the element response. Coleman and Spacone proposed an additional correction procedure to reestablish objectivity of the section response under this approach.

To address this inconsistency of Gauss–Lobatto integration, the modified Gauss–Radau integration method is used with a prescribed plastic hinge length for the bridge pier and the nominal concrete properties. Two approaches to determine l_p are demonstrated. First, l_p is computed as $0.216L$ (=356 mm) from the empirical expression of Paulay and Priestley in Eq. (10). In the second case, l_p is estimated by Eq. (9) to be $0.226L$(=373 mm) for the condition of constant energy release in the confined concrete. The pier response for the modified Gauss–Radau integration method with these plastic hinge lengths is shown in Fig. 12(a), where the computed response accurately represents the cyclic envelope of the experiment.

The moment-curvature response at the base of the pier is shown in Fig. 12(b), where objectivity is maintained for the modified Gauss–Radau plastic hinge integration, in contrast to the nonobjective section response for the regularized Gauss–Lobatto integration. Thus, by incorporating a plastic hinge length, the new integration method ensures objective element response without compromising the section response. The plastic rotation of the bridge pier, computed by Eq. (18), is shown in Fig. 13. When the lateral load capacity of the bridge pier decreases by 20% due to strain softening in the concrete, the plastic rotation is θ^p=0.04.

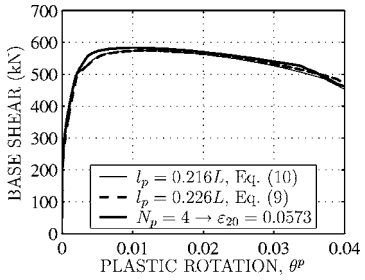

Fig. 13. Plastic rotation at base of reinforced concrete bridge pier with: (i) modified Gauss–Radau plastic hinge integration with l_p computed by Eq. (10); (ii) modified Gauss–Radau plastic hinge integration with l_p computed by Eq. (9); and (iii) four-point Gauss–Lobatto integration with modified concrete properties

Conclusions

A new plastic hinge integration method based on modified Gauss–Radau quadrature has been developed to overcome the difficulties that arise with Gauss–Lobatto integration for strain-softening behavior in force-based beam–column finite elements. The integration method confines material nonlinearity to the element ends over specified plastic hinge lengths, maintains the correct numerical solution for linear curvature distributions, and ensures objective response at the section, element, and structural levels. Plastic rotations are directly related to plastic curvature through the specified plastic hinge lengths. The examples show the modified Gauss–Radau plastic hinge integration method to be a straightforward means of incorporating a physically meaningful plastic hinge length in simulating the strain-softening response of frame structures using force-based beam–column elements. Although results are shown for a pushover analysis, the new plastic hinge integration method can be used for arbitrary loading of an element, including cyclic loads. With the force-based beam–column formulation, it is not possible for a single element integration method to represent both the spread of plasticity under hardening and have objective member and section response under softening. The force-based beam–column element with the new plastic hinge integration method is thus recommended for the nonlinear analysis of frame structures when softening and degradation of the members is expected.

Acknowledgment

This work and the development of *OpenSees* has been supported by the Pacific Earthquake Engineering Research Center under Grant No. EEC-9701568 from the National Science Foundation to the University of California, Berkeley, Calif.

Notation

The following symbols are used in this paper:

b = section force interpolation matrix;

e = section deformation vector;

$\mathbf{f}$ = element flexibility matrix;
$\mathbf{f}^e$ = elastic element flexibility matrix;
$\mathbf{f}^e_{\text{int}}$ = elastic flexibility matrix of element interior;
$\mathbf{f}_s$ = section flexibility matrix;
$\mathbf{f}^e_s$ = elastic section flexibility matrix of element interior;
$\mathbf{k}$ = element stiffness matrix in basic system;
$\mathbf{k}^e$ = elastic element stiffness matrix in basic system;
$\mathbf{k}_s$ = section stiffness matrix;
l_p = plastic hinge length;
N_p = number of element integration points;
$\mathbf{q}$ = element basic force vector;
$\mathbf{s}$ = section force vector;
$\mathbf{v}$ = element deformation vector;
ξ = integration point location; and
ω = integration point weight.

References

Bazant, Z. P., and Planas, J. (1998). *Fracture and size effect in concrete and other quasibrittle materials*, CRC, Boca Raton, Fla.

Clough, R. W., Benuska, K. L., and Wilson, E. L. (1965). "Inelastic earthquake response of tall buildings." *Proc., 3rd World Conf. on Earthquake Engineering*, Wellington, New Zealand.

Coleman, J., and Spacone, E. (2001). "Localization issues in force-based frame elements." *J. Struct. Eng.*, 127(11), 1257–1265.

de Borst, R., Feenstra, P. H., Pamin, J., and Sluys, L. J. (1994). "Some current issues in computational mechanics of concrete structures." *Computer Modelling of Concrete Structures, Proc., EURO-C*, H. Mang, N. Bićanić, and R. de Borst, eds., Swansea, U.K.

El-Tawil, S., and Deierlein, G. G. (1998). "Stress-resultant plasticity for frame structures." *J. Eng. Mech.*, 124(12), 1360–1370.

Federal Emergency Management Agency (FEMA). (2000). "Prestandard and commentary for the seismic rehabilitation of buildings." *FEMA 356*, Washington, D. C.

Filippou, F. C., and Fenves, G. L. (2004). "Methods of analysis for earthquake-resistant structures." *Earthquake engineering: From engineering seismology to performance-based engineering*, Y. Bozorgnia and V. V. Bertero, eds., Chap. 6, CRC, Boca Raton, Fla.

Giberson, M. F. (1967). "The response of nonlinear multistory structures subjected to earthquake excitation." PhD thesis, California Institute of Technology, Pasadena, Calif.

Hildebrand, F. B. (1974). *Introduction to numerical analysis*, McGraw-Hill, New York.

Hilmy, S. I., and Abel, J. F. (1985). "A strain-hardening concentrated plasticity model for nonlinear dynamic analysis of steel buildings." *NUMETA85, Numerical methods in engineering, theory and applications*, Vol. 1, 305–314, Rotterdam, Boston.

Hughes, T. J. R. (1987). *The finite element method*, Prentice-Hall, Englewood Cliffs, N.J.

Kent, D. C., and Park, R. (1971). "Flexural members with confined concrete." *J. Struct. Div. ASCE*, 97(7), 1969–1990.

Mander, J. B., Priestley, M. J. N., and Park, R. (1988). "Theoretical stress–strain model for confined concrete." *J. Struct. Eng.*, 114(8), 1804–1826.

McKenna, F., Fenves, G. L., Scott, M. H., and Jeremić, B. (2000). "Open system for earthquake engineering simulation ⟨http://opensees.berkeley.edu⟩

Neuenhofer, A., and Filippou, F. C. (1997). "Evaluation of nonlinear frame finite-element models." *J. Struct. Eng.*, 123(7), 958–966.

Paulay, T., and Priestley, M. J. N. (1992). *Seismic design of reinforced concrete and masonry buildings*, Wiley, New York.

Powell, G. H., and Chen, P. F. (1986). "3D beam-column element with generalized plastic hinges." *J. Eng. Mech.*, 112(7), 627–641.

Simo, J. C., and Hughes, T. J. R. (1998). *Computational inelasticity*, Springer-Verlag, New York.

Spacone, E., Ciampi, V., and Filippou, F. C. (1996). "Mixed formulation of nonlinear beam finite element." *Comput. Struct.*, 58, 71–83.

Stoer, J., and Bulirsch, R. (1993). *Introduction to numerical analysis*, 2nd Ed., Springer, New York.

Tanaka, H., and Park, R. (1990). "Effect of lateral confining reinforcement on the ductile behaviour of reinforced concrete columns." *Rep. No. 90-2*, Dept. of Civil Engineering, Univ. of Canterbury, Canterbury, U.K.

Zienkiewicz, O. C., and Taylor, R. L. (2000). *The finite element method: The basis*, 5th Ed., Vol. 1, Butterworth, Stoneham, Mass.